Effects of magnetic field on the two-dimensional systems of antiferromagnetically correlated electrons based on the Hubbard model Hamiltonian with easy axis: Aharonov-Bohm and Zeeman effects

Seung-Pyo Hong,[1] Sung-Sik Lee,[1] and Sung-Ho Suck Salk[2]
[1]*Department of Physics, Pohang University of Science and Technology, Pohang 790-784, Korea*
[2]*Korea Institute of Advanced Studies, Seoul 130-012, Korea*
(Received 12 March 1999; revised manuscript received 30 June 2000)

In the present study we study the two-dimensional systems of antiferromagnets with easy axis and the variation of staggered magnetization with the increase of magnetic fields. The Aharonov-Bohm and the Zeeman effects on the staggered magnetizations are examined. The reentrant behavior of paramagnetic phase is shown to occur even at extremely high applied magnetic fields when only the Aharonov-Bohm effect is taken into account. An inhomogeneous phase (i.e., the inhomogeneous distribution with antiferromagnetic clusters) is also shown to exhibit the reentrant behavior. On the other hand, when the Zeeman effect is introduced, the reentrant behavior occurs only at low fields below a critical magnetic field corresponding to a critical Zeeman energy close to the hopping energy in the order of magnitude.

I. INTRODUCTION

Earlier various studies were made for the two-dimensional (2D) systems of noninteracting electrons under external magnetic field. [1–3] Recently one among the interesting subjects is concerned with the effects of the external magnetic field on the systems of interacting electrons. Held *et al.*[4] studied the microscopic origin of metamagnetism for antiferromagnets in the external magnetic field, by applying the dynamical mean-field theory to the Hubbard model. Bagehorn and Hetzel[5] observed the second-order phase transition at zero temperature from the projector quantum Monte Carlo calculation of the Hubbard model with an easy axis. Earlier we[6,7] investigated the variation of staggered magnetization with the external magnetic field for the two-dimensional systems of antiferromagnetically correlated electrons, at half-filling (i.e., no hole doping) and at zero temperature. The objective of the present paper is twofold; one is to investigate for the hole-doped systems the effects of the Aharonov-Bohm phase on the phase diagram of staggered magnetization in the plane of temperature versus hole doping rate, and the other is to study the influence of the Zeeman coupling on the staggered magnetization (antiferromagnetic order) for the two-dimensional antiferromagnets with easy axis.

II. AHARONOV-BOHM EFFECTS

We write the Hubbard model Hamiltonian describing the two-dimensional system of antiferromagnetically correlated electrons under an external magnetic field,[3]

$$H=-t\sum_{\langle ij\rangle\sigma}\left[\exp\left(-i\frac{2\pi}{\phi_0}\int_j^i \mathbf{A}\cdot dl\right)c_{i\sigma}^{\dagger}c_{j\sigma}+\text{H.c.}\right]+U\sum_i n_{i\uparrow}n_{i\downarrow}-\mu\sum_{i\sigma}c_{i\sigma}^{\dagger}c_{i\sigma}, \tag{1}$$

where t is the hopping integral; $\mathbf{A}$ is the electromagnetic vector potential; $\phi_0=hc/e$, is the elementary flux quantum. The electron acquires the Aharonov-Bohm phase when hopping to the nearest-neighbor sites. U is the on-site Coulomb repulsion energy and μ is the chemical potential. $\langle ij\rangle$ stands for summation over nearest-neighbor sites i and j. $c_{i\sigma}^{\dagger}$ ($c_{i\sigma}$) is the creation (annihilation) operator of an electron of spin σ at site i, and $n_{i\uparrow}$ ($n_{i\downarrow}$), the number operator of an up-spin (down-spin) electron at site i.

In the present study we allow a uniform (site-independent) staggered magnetization and a uniform doping rate,

$$m=\frac{1}{N}\sum_{i\sigma}e^{i\mathbf{Q}\cdot\mathbf{r}_i}\sigma\langle c_{i\sigma}^{\dagger}c_{i\sigma}\rangle, \tag{2a}$$

$$\delta=1-\frac{1}{N}\sum_i\langle n_i\rangle, \tag{2b}$$

with $\mathbf{Q}=(\pi,\pi)$ and $\sigma=+1(-1)$ for spin-up (spin-down). Here $\mathbf{r}_i=(i_x,i_y)$ with i_x and i_y being integers with the lattice spacing of unity, and N is the number of lattice sites. For the Ising antiferromagnet of present interest, the Mermin-Wagner theorem does not apply since the Ising system shows spontaneous magnetization in a finite-temperature interval. It is noted that earlier Onsager[8] and Yang[9] analyzed the critical behavior of the two-dimensional Ising model on a square lattice.

Introducing the mean-field (Hartree-Fock) approximation and using the Landau gauge $\mathbf{A}=B(0,x,0)$, we obtain, in momentum space,

$$H=-t\sum_{\mathbf{k}\sigma}\left[2\cos k_x c_{\mathbf{k}\sigma}^{\dagger}c_{\mathbf{k}\sigma}+e^{-ik_y}c_{\mathbf{k}-\mathbf{g},\sigma}^{\dagger}c_{\mathbf{k}\sigma}+e^{ik_y}c_{\mathbf{k}+\mathbf{g},\sigma}^{\dagger}c_{\mathbf{k}\sigma}\right]-\frac{mU}{2}\sum_{\mathbf{k}\sigma}\sigma c_{\mathbf{k}+\mathbf{Q},\sigma}^{\dagger}c_{\mathbf{k}\sigma}-h\sum_{\mathbf{k}\sigma}\sigma c_{\mathbf{k}\sigma}^{\dagger}c_{\mathbf{k}\sigma}+\left[\frac{U}{2}(1-\delta)-\mu\right]\sum_{\mathbf{k}\sigma}c_{\mathbf{k}\sigma}^{\dagger}c_{\mathbf{k}\sigma}, \tag{3}$$

where $\mathbf{g}\equiv(2\pi\phi/\phi_0,0)=(2\pi p/q,0)$ with p/q being the number of flux quanta per plaquette. The first term in Eq. (3) represents hopping processes; the first term in the bracket represents the nearest-neighbor hopping in the x direction and the last two terms in the bracket are the nearest-neighbor hopping in the y direction. The electromagnetic vector potential $\mathbf{A}$ shifts the wave vector of electron by $g\equiv|\mathbf{g}|=2\pi p/q$ in the x direction. The second term results from the antiferromagnetic order which shifts the wave vector by $\mathbf{Q}$. The last term shifts the total energy of the system as a result of hole doping. The exchange terms that appear in the Hartree-Fock approximation vanish due to the constraint of the global SU(2) symmetry for the square lattice of the antiferromagnetically correlated electrons.

The diagonalization of Eq. (3) leads to the following generalized Harper's equation:

$$\det(\mathbf{H}_{k\sigma}-E_k\mathbf{I})=0 \tag{4a}$$

with

$$\mathbf{H}_{k\sigma}=\begin{bmatrix}\mathbf{T}_k & \mathbf{V}_\sigma\\ \mathbf{V}_\sigma & -\mathbf{T}_k\end{bmatrix}, \tag{4b}$$

where

$$\mathbf{T}_k=-t\begin{bmatrix} M_1 & e^{-ik_y} & 0 & 0 & e^{ik_y}\\ e^{ik_y} & M_2 & \ddots & 0 & 0\\ 0 & \ddots & \ddots & \ddots & 0\\ 0 & 0 & \ddots & M_{q-1} & e^{-ik_y}\\ e^{-ik_y} & 0 & 0 & e^{ik_y} & M_q\end{bmatrix}, \tag{4c}$$

with $M_n=2\cos(k_x+ng)$, and

$$\mathbf{V}_\sigma=\begin{bmatrix} -\frac{\sigma mU}{2} & 0 & 0 & 0 & 0\\ 0 & -\frac{\sigma mU}{2} & 0 & 0 & 0\\ 0 & 0 & \ddots & 0 & 0\\ 0 & 0 & 0 & -\frac{\sigma mU}{2} & 0\\ 0 & 0 & 0 & 0 & -\frac{\sigma mU}{2}\end{bmatrix}. \tag{4d}$$

Here the matrix $\mathbf{T}_k$ associated with electron hopping contains information on the phase modulation of hopping electrons under the influence of the external field; $\mathbf{V}_\sigma$, is the antiferromagnetic electron correlations, and $\mathbf{I}$, is the identity matrix. E_k is the quasiparticle dispersion energy of the antiferromagnetically correlated electrons in the presence of magnetic field. We obtain the dispersion energy of the interacting electrons from the diagonalization of the Hamiltonian matrix $\mathbf{H}_{k\sigma}$ in Eq. (4b) above,

$$E_k=\sqrt{\varepsilon_k^2+\Delta^2}, \tag{5}$$

with the bang gap, $2\Delta=mU$. Here ε_k is the dispersion energy of noninteracting electrons in the presence of magnetic field; $\varepsilon_k=-2t\sqrt{\cos^2k_x+\cos^2k_y}$ for $p/q=1/2$, and $\varepsilon_k=-2t(\cos k_x+\cos k_y)$ for $p/q=0$.

The staggered magnetization m and the chemical potential μ vary with both the temperature T and the hole doping rate (concentration) δ. They are obtained from the use of self-consistent mean-field equations: we first write Eqs. (2a) and (2b) in terms of quasiparticle operators in momentum space and then use the Fermi-Dirac distribution function for the quasiparticles (fermions), to finally obtain

$$1=\int dE g(E)\frac{U}{8|E|}\left[\tanh\frac{E^{(+)}}{2T}-\tanh\frac{E^{(-)}}{2T}\right], \tag{6a}$$

$$\delta=\int dE\frac{g(E)}{4}\left[\tanh\frac{E^{(+)}}{2T}+\tanh\frac{E^{(-)}}{2T}\right], \tag{6b}$$

where $E^{(\pm)}=\pm E+U/2(1-\delta)-\mu$. Here $g(E)$ is the density of states for the electrons, which can be obtained from

$$g(E)=2\int'\frac{d^2k}{(2\pi)^2}\delta(E-E_k). \tag{7}$$

The integration $\int' d^2k$ is over the reduced Brillouin zone of $(k_x,k_y)\,|-\pi/q\leq k_x\leq\pi/q$ and $-\pi/2\leq k_y\leq\pi/2$. The Brillouin zone is reduced by $1/q$ in the k_x direction because there exist q plaquettes per magnetic unit cell, and its area is further reduced by 1/2 as a result of the antiferromagnetic ordering.

Earlier, only for the case of zero magnetic field, a reentrant behavior was discovered by other investigators;[10–12] Halvorsen *et al.*[11] found the reentrant behavior using the Hubbard model in infinite dimensions within the self-consistent second-order weak U-perturbation treatment, and Inaba *et al.*[12] also obtained a similar reentrant behavior, by using the slave-boson approach to the t-J Hamiltonian. However, all of these studies are limited to the case of zero field. It is thus of great interest to see how the externally applied magnetic field affects the reentrant behavior and the phase diagram. To incorporate the Aharonov-Bohm effect it is necessary to choose a sufficiently large size of square lattice to meet the periodic boundary conditions of magnetic unit cells which correspond to various values of magnetic fields (or p/q). For this study we have to choose the mean-field Hubbard model calculations since the accurate exact diagonalization (Lanczos) method is presently limited to only a small-size lattice. In order to examine the dependence of staggered magnetization m on the external magnetic field in the plane of temperature T versus doping rate δ we solve numerically the analytically derived self-consistent mean-field equations of Eqs. (6a) and (6b) above. Figure 1 displays the predicted staggered magnetization (antiferromagnetic order) between two cases, i.e., one in the presence of the external field (dotted lines) and the other in the absence of the external field (solid line). The region below each solid curve represents the antiferromagnetic phase and the region above it, the paramagnetic phase. We find that the incorporation of the Aharonov-Bohm phase reduces the antiferromagnetic region in the phase diagram and does not destroy the reentrant behavior of the paramagnetic phase (follow the arrow in the figure to see the reentrant behavior showing the transition from a paramagnetic region to an antiferromagnetic region to

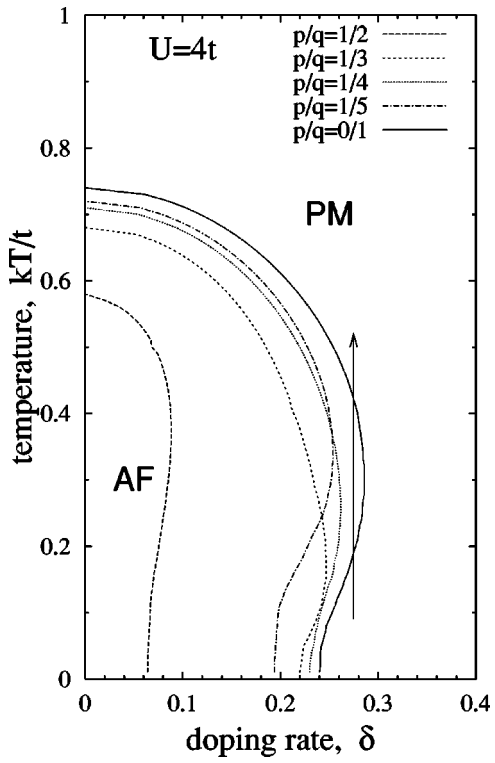

FIG. 1. Phase diagram of staggered magnetization for several values of magnetic flux quanta per plaquette p/q in the (T,δ) plane with $U=4t$. Boundaries between the antiferromagnetic (AF) phase and the paramagnetic (PM) phase are indicated by various curves. The arrow is a guide for the reentrant behavior of the paramagnetic phase.

another paramagnetic region as temperature increases) even in the presence of the applied magnetic field.

In Fig. 2 we display the temperature dependence of the staggered magnetization for various doping rates. At half filling ($\delta=0$) the staggered magnetization reaches a maximum at zero temperature. On the other hand, away from half filling ($\delta\neq 0$) the predicted staggered magnetization shows a maximum at a finite temperature. Above this temperature the reentrant behavior of the paramagnetic phase is observed. The reentrant behavior occurs by exhibiting a maximum

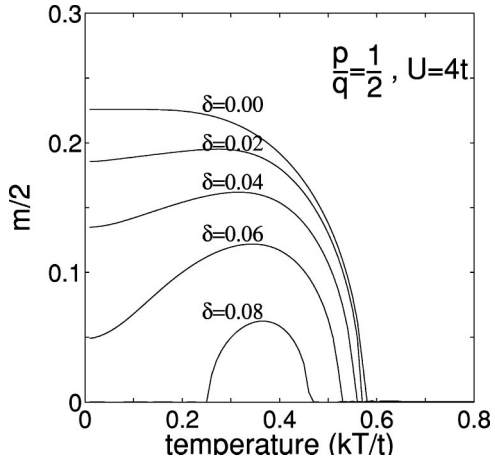

FIG. 2. Temperature dependence of staggered magnetization with $p/q=1/2$ for various values of doping rates.

value in the staggered magnetization at finite temperatures. This can be explained from the nesting property of the energy surface at saddle points.[7,12] In Fig. 3 we display the variation of the energy dispersion of the highest occupied subband as the external magnetic field (or p/q) changes. The saddle points in the Brillouin zone are denoted by black dots at the bottom of the graph. The adjacent saddle points are separated by the well-defined nesting vector of $\mathbf{Q}/q$, by which the staggered magnetization is defined. At the bottom of the graphs in Fig. 3 we display the variation of Fermi surface (contour lines) with the magnetic field at finite doping rates and at zero temperature. As is shown in the figures, the Fermi surface at zero temperature is predicted to have a poor nesting property and consequently the staggered magnetization is expected to be small. As the temperature increases, the Fermi surface tends to smear out, which allows increment in the number of nesting channels. As a consequence the staggered magnetization will increase. As the temperature further increases, the Fermi surface nesting may eventually disappear. As a result the staggered magnetization will eventually disappear to allow a transition to a paramagnetic phase. This is the reentrant behavior for the homogeneous phase which is well displayed in Fig. 1.

So far we have considered the case of homogeneous solutions, i.e., the uniform staggered magnetization. It is known that the Hartree-Fock approximation for the 2D Hubbard model leads to inhomogeneous solutions for the systems of correlated electrons away from half-filling. [13–15] For the illustration of such an inhomogeneous solution we performed self-consistent mean-field calculations on a 12×12 lattice with periodic boundary conditions, by choosing the hole doping concentration of $\delta\simeq 0.1$ ($\delta=14/144$) at $T=0.1t$. The predicted inhomogeneous phase is shown in Fig. 4(a). Phase separation is observed to occur between the hole-rich regions and the hole-free regions of an antiferromagnetic order. Since the system does not have a homogeneous long-range antiferromagnetic order with momentum $\mathbf{Q}$, we introduce a magnetic order parameter defined by

$$m_a=\frac{1}{N}\sum_i |\langle S_i^z\rangle|. \tag{8}$$

Although the nesting vector $\mathbf{Q}$ does not appear in Eq. (8), m_a can be used as a measure of local antiferromagnetic order for the system of the inhomogeneous phase which consists of locally antiferromagnetic clusters separated by hole-rich regions. In Fig. 4(b), the calculated m_a is shown as a function of temperature. Interestingly enough, with the external magnetic field of $p/q=1/2$, m_a is predicted to show a maximum at a finite temperature, similarly to the case of homogeneous phase shown in Fig. 2 for various hole doping rates. This indicates the existence of the reentrant behavior even in the case of the inhomogeneous phase.

III. ZEEMAN EFFECTS

With the inclusion of Zeeman coupling term, the two-dimensional Hubbard model Hamiltonian is written

$$H=-t\sum_{\langle ij\rangle\sigma}(c_{i\sigma}^{\dagger}c_{j\sigma}+\text{H.c.})+U\sum_i n_{i\uparrow}n_{i\downarrow}-h\sum_{i\sigma}\sigma c_{i\sigma}^{\dagger}c_{i\sigma}, \tag{9}$$

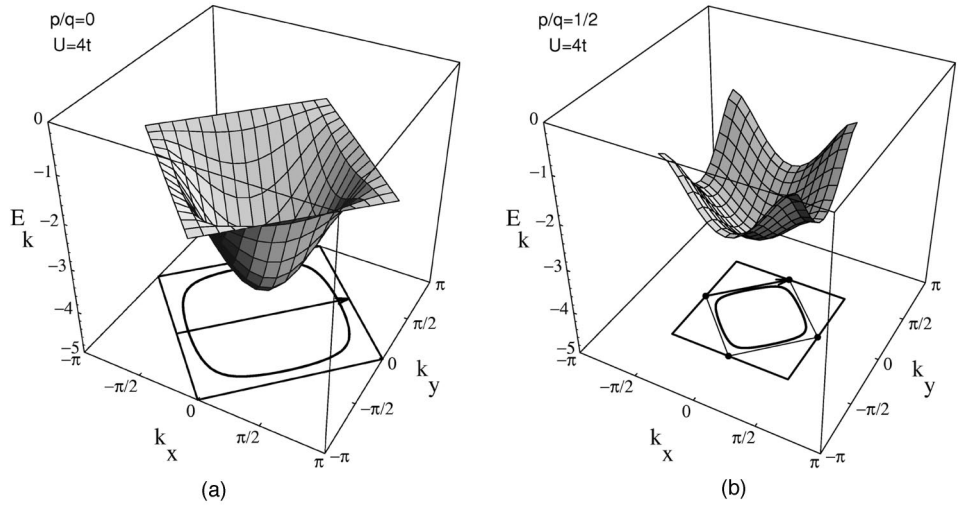

FIG. 3. Variation of quasiparticle energy dispersion surface of the highest occupied subband with various values of p/q. Black dots denote the saddle points of the surface. Rectangles at the bottom of each graph represent the reduced Brillouin zones, and arrows are the nesting vectors between two adjacent saddle points. The thick contour lines are Fermi surfaces at zero temperature and at various hole-doping rates: (a) $\delta = 0.33$, (b) $\delta = 0.30$.

where h is the Zeeman energy and $\sigma = +1(-1)$ for up (down) spin. For an accurate account of the Zeeman effect for the systems of correlated electrons, the above Hamiltonian will be diagonalized by applying the Lanczos exact diagonalization method to a tilted $\sqrt{10}\times\sqrt{10}$ square lattice with periodic boundary conditions. For the small size of square lattice above (owing to current difficulty of using a sufficiently large size of square lattice), the exact diagonalization treatment yields inaccurate accounts of the Aharonov-Bohm effects owing to the failure of meeting the periodic boundary conditions with various sizes of magnetic unit cells. Thus we focus only on the effect of the Zeeman coupling.

For the exact diagonalization treatment, the uniform $[q = (0,0)]$ and staggered $[Q = (\pi,\pi)]$ magnetization is defined by[16]

$$\langle (\mathbf{m}_q)^2 \rangle = \left\langle \left(\frac{1}{N} \sum_i e^{i\mathbf{q}\cdot\mathbf{r}_i} \mathbf{S}_i \right)^2 \right\rangle. \tag{10}$$

Here $(\mathbf{m}_q)^2$ represents the square of the uniform and the staggered magnetizations corresponding to $q = (0,0)$ and $q = Q \equiv (\pi,\pi)$, respectively. We show the predicted magnetization with $U = 4t$ as a function of the applied field in Fig. 5. Appearance of the stepwise curves is inevitable due to the finite-size effect. This is because owing to the small size lattice the difference in number between the up ($N_\uparrow$) and down ($N_\downarrow$) spins discretely varies with the change of magnetic field, e.g., $N_\uparrow - N_\downarrow = 0,2,\ldots,10$ for the small size of the half-filled $\sqrt{10}\times\sqrt{10}$ lattice. As the number of lattice sites and thus the number of electron spins increases, the stepwise curves are expected to gradually disappear. For a relatively low magnetic field corresponding to the Zeeman energy below $h \lesssim 0.3t$, we find that antiferromagnetic correlations (staggered magnetizations) are present with no net uniform magnetization. For the Zeeman energy in the range of $0.3t \lesssim h \lesssim 0.6t$, the mixed phase of the staggered magnetization and the uniform magnetization appears. In this range the uniform magnetization rapidly increases while the staggered magnetization appreciably decreases. This indicates that the phase transition is of second order by showing the mixed phase, as is displayed in Fig. 5. Although not shown here, a similar behavior is observed for the case of weaker electron correlations, i.e., the Coulomb repulsion of $U < 4t$. The phase transition tends to occur at a critical Zeeman energy, $h_c \simeq 0.6t$ below a lower hopping energy.

Now, with the introduction of only the Zeeman effects in the Hartree-Fock calculations, Fig. 6 displays the magnetization as a function of the Zeeman energy. The quantitative difference between the Hartree-Fock and the exact diagonalization results is observed in that the critical Zeeman energy appears at a larger value compared to the exact diagonalization result. However in both methods the critical Zeeman energy h_c is found to be close to the hopping energy t in the order of magnitude (with $h_c \simeq 0.6t$ for the exact diagonalization method and $h_c \simeq 1.2$ for the Hartree-Fock method). Despite the quantitative differences, a similar trend in the reentrant behavior is observed with the fields below a critical magnetic field. Unlike the case of the exact diagonalization, it is found that the phase transition is of first order, showing no distinctive mixed phase of the staggered magnetization (antiferromagnetic order) and the uniform magnetization. Now, as is shown in Fig. 7 the inclusion of both the Aharonov-Bohm and the Zeeman effects shows a similar feature with nearly the same critical Zeeman energy to the result obtained only for the Zeeman effects (see Fig. 6). For completeness, only with the inclusion of the Aharonov-Bohm effects does Fig. 8 display the persistence of the staggered magnetization (antiferromagnetic order), even at very high fields. This is why there exists the persistence of the reentrant behavior even at extremely high magnetic fields, as is shown in Figs. 1 and 2.

We estimate the Zeeman energies corresponding to the various magnetic flux quanta p/q. Choosing the lattice spacing a as the nearest-neighbor Cu-Cu distance in the high-T_c cuprates, e.g., $a \simeq 3.5$ Å for $La_{2-x}Sr_xCuO_4$,[17] the estimated Zeeman energy is

$$h = \mu_B B = \mu_B \frac{\phi_0(p/q)}{a^2} \simeq 2.0 \frac{p}{q} \text{ eV}, \tag{11}$$

where μ_B is the Bohr magneton. For the choice of the hopping energy of $t \simeq 0.4$ eV obtained from a local-density-functional calculation,[18] the magnetic fields associated with the flux quanta above $p/q = 1/5$ correspond to the Zeeman

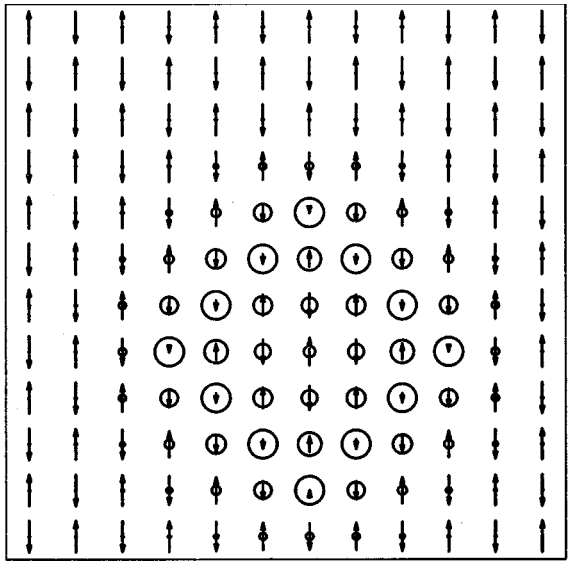

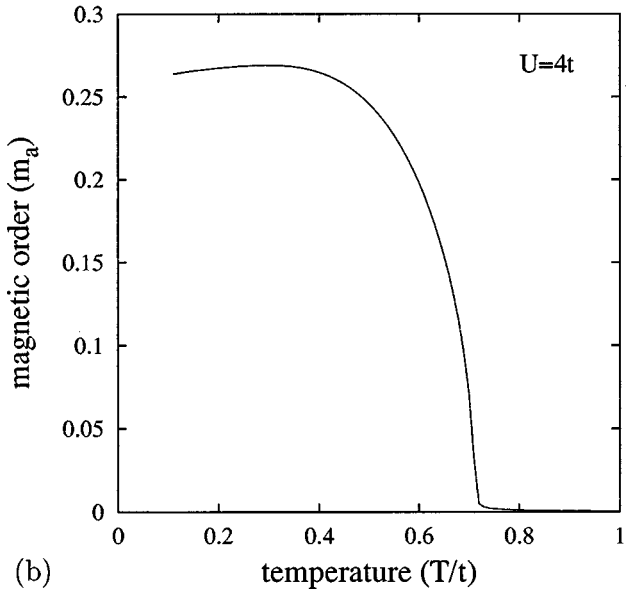

FIG. 4. (a) Illustration of an inhomogeneous phase with the hole doping rate, $\delta \simeq 0.1$ (14/144) at $T=0.1t$ and $U=4t$. The length of arrow at each site indicates the magnitude of spin and the size of circle denotes the magnitude of hole charge density. (b) m_a (a measure of local antiferromagnetic order) as a function of temperature with $p/q=1/2$.

energies greater than the hopping energy. Indeed, the the antiferromagnetic order (staggered magnetization) tends to disappear at such high magnetic fields, as are well displayed in Figs. 5–7. Thus, with the introduction of the Zeeman effects the reentrant behavior is expected to occur only with fields below the critical magnetic field h_c which corresponds to the Zeeman energy close to the hopping energy t in the order of magnitude.

IV. CONCLUSION

In the present study, by applying the self-consistent Hartree-Fock mean-field method to the two-dimensional an-

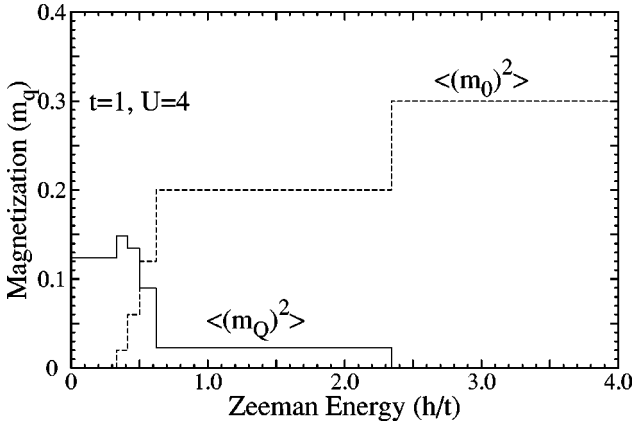

FIG. 5. Staggered (solid line) and uniform (dotted line) magnetizations as a function of Zeeman energy based on the exact diagonalization (Lanczos) method.

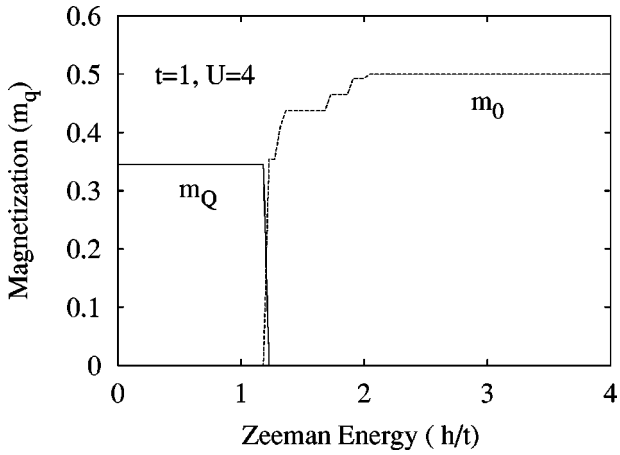

FIG. 6. Staggered (solid line) and uniform (dotted line) magnetizations as a function of Zeeman energy based on the self-consistent Hartree-Fock method with the consideration of only the Zeeman effect with $U=4t$.

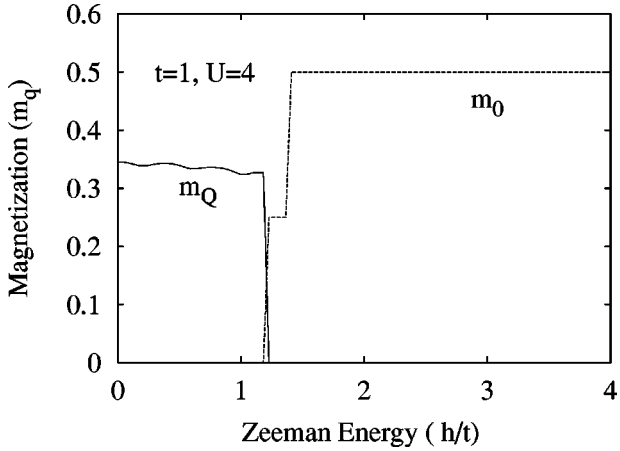

FIG. 7. Staggered (solid line) and uniform (dotted line) magnetizations as a function of Zeeman energy based on the self-consistent Hartree-Fock method with the consideration of both the Aharonov-Bohm and the Zeeman effects with $U=4t$.

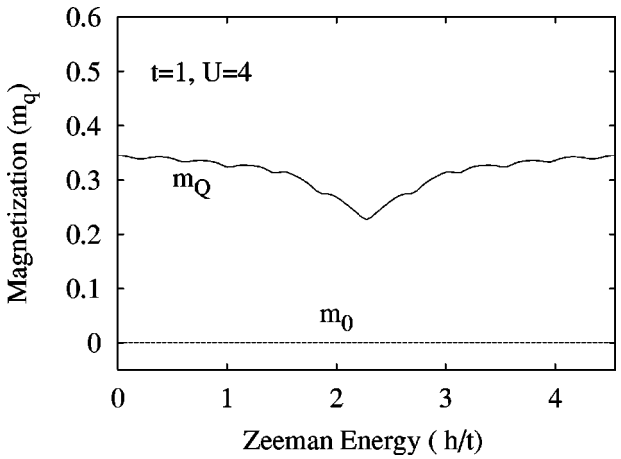

FIG. 8. Staggered (solid line) and uniform (dotted line) magnetizations as a function of Zeeman energy based on the self-consistent Hartree-Fock method with the consideration of only the Aharonov-Bohm effect with $U=4t$.

tiferromagnets, we examined both the phase diagram of the staggered magnetization (antiferromagnetic order) in the (T,δ) plane as a function of magnetic flux quantum (magnetic field) and the magnetization as a function of the Zeeman energy. We find that for the homogeneous phase the Aharonov-Bohm effect causes a reduction of the antiferromagnetic region in the phase diagram (see Fig. 1). The reentrant behavior of the paramagnetic phase is observed even at extremely high magnetic fields corresponding to $p/q=1/2$. We also noted that the phase-separated inhomogeneous system [see Fig. 4(a)] allows the reentrant behavior [see Fig. (4(b)] similarly to the case of the homogeneous antiferromagnetic systems (see Figs. 1 and 2). However, unlike the above cases, with the inclusion of only the Zeeman effects the reentrant behavior is expected to occur only with low fields below a critical magnetic field corresponding to a critical Zeeman energy close to the hopping energy in the order of magnitude. Both the Hartree-Fock and the exact diagonalization methods yielded a similar critical Zeeman energy in the order of magnitude. However, it is found that the predicted phase transition by the Hartree-Fock method is of first order while it is of second order by the exact diagonalization method. The inclusion of both the Aharonov-Bohm and the Zeeman effects yielded similar results to the above case.

ACKNOWLEDGMENTS

S.-H.S.S. acknowledges the financial support of the Korean Ministry of Education BSRI (1998) and POSTECH/BSRI. He is also grateful to the SRC program (1998) of the Center for Molecular Science at KAIST. We are grateful to Chan-Ho Yang for computational assistance.

[1] D. Hofstadter, Phys. Rev. B **14**, 2239 (1976).
[2] A. H. MacDonald, Phys. Rev. B **28**, 6713 (1983).
[3] Y. Hasegawa, P. Lederer, T. M. Rice, and P. B. Wiegmann, Phys. Rev. Lett. **63**, 907 (1989).
[4] K. Held, M. Ulmke, N. Blümer, and D. Vollhardt, Phys. Rev. B **56**, 14 469 (1997), and references therein.
[5] F. Bagehorn and R. E. Hetzel, Phys. Rev. B **56**, R10 005 (1997), and references therein.
[6] H. Doh, S. P. Hong, and S. H. Salk, Phys. Rev. B **55**, 14 084 (1997); H. Doh and S. H. S. Salk, Physica C **263**, 86 (1996); J. Korean Phys. Soc. **28**, S588 (1995).
[7] S.-P. Hong, H. Doh, and S.-H. S. Salk, Physica C **282-287**, 1697 (1997); Czech. J. Phys. **46**, Suppl. S4, 1855 (1996).
[8] L. Onsager, Phys. Rev. **65**, 117 (1949).
[9] C. N. Yang, Phys. Rev. **85**, 809 (1952).
[10] Y. Hasegawa and H. Fukuyama, Jpn. J. Appl. Phys., Part 2 **26**, L322 (1987).
[11] E. Halvorsen and G. Czycholl, J. Phys.: Condens. Matter **6**, 10 331 (1994).
[12] M. Inaba, H. Matsukawa, M. Saitoh, and H. Fukuyama, Physica C **257**, 299 (1996).
[13] H. J. Schulz, Phys. Rev. Lett. **64**, 1445 (1990).
[14] D. Poilblanc and T. M. Rice, Phys. Rev. B **39**, 9749 (1989).
[15] J. A. Vergés, E. Louis, P. S. Lomdahl, F. Guinea, and A. R. Bishop, Phys. Rev. B **43**, 6099 (1991).
[16] E. Dagotto and A. Moreo, Phys. Rev. B **38**, 5087 (1988).
[17] E. Dagotto, Rev. Mod. Phys. **66**, 763 (1994).
[18] M. S. Hybertsen, E. B. Stechel, M. Schluter, and D. R. Jennison, Phys. Rev. B **41**, 11 068 (1990).